

Spectral properties of exciton polaritons in one-dimensional resonant photonic crystals

M. V. Erementchouk, L. I. Deych, and A. A. Lisyansky

Physics Department, Queens College, City University of New York, Flushing, New York 11367, USA

(Received 30 November 2005; revised manuscript received 6 February 2006; published 20 March 2006)

The dispersion properties of exciton polaritons in multiple-quantum-well-based resonant photonic crystals are studied. In the case of structures with an elementary cell possessing a mirror symmetry with respect to its center, a powerful analytical method for deriving and analyzing dispersion laws of the respective normal modes is developed. The method is used to analyze band structure and dispersion properties of several types of resonant photonic crystals, which would not submit to analytical treatment by other approaches. These systems include multiple-quantum-well structures with an arbitrary periodic modulation of the dielectric function and structures with a complex elementary cell. Special attention was paid to determining conditions for superradiance (Bragg resonance) in these structures and to the properties of the polariton stop band in the case when this condition is fulfilled (Bragg structures). The dependence of the band structure on the angle of propagation, the polarization of the wave, and the effects due to exciton homogeneous and inhomogeneous broadenings are considered, as well as dispersion properties of excitations in near-Bragg structures.

DOI: [10.1103/PhysRevB.73.115321](https://doi.org/10.1103/PhysRevB.73.115321)

PACS number(s): 42.25.Dd, 72.15.Rn, 05.40.-a, 71.55.Jv

I. INTRODUCTION

Optical properties of artificial structures with periodically modulated dielectric constant have been attracting a great deal of interest since pioneering papers of Refs. 1 and 2, where such systems were first discussed. Periodic modulation of the dielectric function significantly modifies the spectral properties of electromagnetic waves. Instead of a simple continuous spectrum with a linear dispersion law, the electromagnetic spectrum in such structures is characterized by the presence of allowed and forbidden bands similar to the electronic band structure of crystals. For this reason, the new class of optical materials was dubbed photonic crystals.³ Changing the spatial distribution of the dielectric constant one can effectively control such fundamental properties as the group velocity of light, the rate of spontaneous emission, etc. This fact has important repercussions for both fundamental physics and applications, where it opens up possibilities for new concepts of optical and optoelectronic devices.

Modulation of the dielectric function, however, is not the only way to affect light propagation and its interaction with matter. It was shown in Ref. 4 that closely packed dipole-active atoms can become coherently coupled by light and this coupling significantly changes their emission properties, resulting in the so-called “superradiance” effect. In the original Dicke’s model⁴ the distance between the atoms was assumed to be much smaller than the wavelength of their emission, but similar effects can also arise if dipole-active elements form a one-dimensional periodic lattice with the period coinciding with the emission half-wavelength (Bragg resonance). Such an arrangement is possible with a so-called optical lattice of cold atoms⁵ and with their semiconductor analogs—Bragg multiple-quantum-well (MQW) structures.^{6–9} The latter are semiconductor heterostructures, in which very thin layers of a narrower-band-gap semiconductor (quantum well) are separated from each other by much thicker layers of a wider-band-gap semiconductor (barrier) in such a way that the period of the structure coincides with the half-wavelength of light emitted by excitons confined in a

quantum well (QW). In these systems, excitons play the role of the dipole-active excitations, which become radiatively coupled and demonstrate the superradiance effect. If, however, the size (the number of periods) in an optical lattice increases, the properties of the system change.^{10,11} In particular, the dark modes form two branches of collective excitations, in which light is coupled with the material resonances and which can be called optical lattice polaritons. At the same time, the superradiance mode develops into a stop band, which is a spectral gap between the two polariton branches, characterized by almost complete reflection of a normally incident radiation. The distinction between Bragg structures and other arrangements, in which the period of the structure is not in the resonance with radiation emitted by the active elements, can, in this case, be described in terms of formation of a significantly (by orders of magnitude) enhanced stop band.

There is, however, an important difference between optical lattices of atoms and semiconductor heterostructures. In the latter case, the interaction of light with active elements (excitons) is accompanied by multiple reflection of light from interfaces between wells and barrier layers caused by a difference in their refractive indexes. Thus, in structures like MQW’s optical lattice effects coexist with photonic crystal-like effects, which results in a number of interesting optical properties and opportunities for applications. Such structures, called resonant photonic crystals (RPC’s), have recently started attracting significant attention.^{12–19} A general characteristic of this type of structures is the coexistence of dipole-active material excitations (excitons, phonons, plasmons) described by optical susceptibilities of the resonant type and periodic modulation of the background dielectric constant. The two most fundamental problems in the focus of current research in this area are concerned with the effects of the interplay between resonances and spatial nonuniformity of the dielectric function on the band structure of these systems and their optical spectra. While these two questions are interconnected, they have to be recognized as two separate problems, one dealing with normal modes of closed (or infi-

nite) systems and their dispersion laws and the other with the interaction of an internal radiation with a finite-size structure.

The main interest of studies in this field is a spectral region in the vicinity of the resonant frequency, where the interplay effects play the most important role. A theoretical description of RPC's in this spectral region is a challenging problem, and its complete solution has not yet been obtained even for a simplest case of one-dimensional structures, such as MQW's. Of course, it is always possible to carry out numerical calculations of the optical spectra and the dispersion laws, which are particularly easy in the one-dimensional case. However, a purely numerical approach does not provide a real understanding of the physics of these structures. Therefore, it is very important to be able to carry out an analytical analysis, which would not only provide a better understanding of the physical processes taking place in these structures, but would also be instrumental in designing structures with predetermined properties, which is crucial for their possible applications.

Different aspects of this problem have been, of course, considered in a number of previous publications. In particular, in Ref. 20 the necessity of a modification of the Bragg resonance (superradiance) condition for one-dimensional resonant photonic crystals compared to the case of optical lattice structures was shown. Later, this result was confirmed²¹ and an exact Bragg condition in such structures was found for the particular case of normal propagation of the electromagnetic wave. It was also noted in Ref. 21 that, when the resonance condition is met, the spectral gap between the polariton branches becomes wider than in the case of a passive photonic crystal characterized by the same modulation of the dielectric function or of an optical lattice with the same strength of radiative coupling between the active elements. In the case of structures of higher (two or three) dimensions, no analytical results are available yet, but one can note recent numerical calculations presented in Refs. 18 and 22, where it was also found that the resonances may enhance polariton-related band gaps compared to a purely passive photonic crystal with the same spatial distribution of the dielectric constant. It is important to emphasize that this enhancement of the band gap in RPC structures is not a trivial effect. In order to illustrate this point we can mention another, in a certain sense, opposite effect, which also results from the interplay between the resonances and periodic inhomogeneities of the dielectric function. It was shown in Ref. 23 that there always exists a frequency where the reflection coefficient of the incident light vanishes due to the destructive interference between the two channels of interaction between light and the structure.

These examples show the richness of the optical properties of even one-dimensional resonant photonic crystals. In order to achieve a complete understanding of the relationships between the optical and geometrical characteristics of these structures, one needs a general analytical method which could be applied to a variety of RPC's independently of a particular spatial dependence of their dielectric function. In our previous paper, Ref. 23, such a method was developed for studying *reflection, transmission, and absorption spectra* of finite one-dimensional RPC structures. The present paper presents a general analytical approach to calculating the

band structure of these materials. This method allows one to analyze the dispersion laws of one-dimensional RPC's with an arbitrary form of the periodic modulation of the dielectric function, propagation angle of the electromagnetic wave, and its polarization state. The method naturally incorporates resonant excitations of the medium into the theory. For concreteness, we assume that the resonances are related to exciton states in QW's; however, the method can be easily applied to any other type of resonance-localized excitations.

The approach developed in the present paper complements that of Ref. 23, thus completing the development of a general theory of optical spectra and dispersion characteristics of optical properties of MQW-based RPC's. While the main focus of the paper is methodological, we also present here some results concerning the dispersion properties of MQW-based RPC's, which could not be obtained by other methods. For instance, we were able to obtain analytical expressions describing the dispersion laws of electromagnetic waves in such structures with an arbitrary polarization state and an arbitrary value of the in-plane wave number. In particular, we found an interesting effect of the collapse of one of the band gaps and discussed the property of the omnidirectional reflectivity in these structures. We also showed that an idea of a perfect Bragg arrangement can be realized in more complex structures such as MQW's with complex elementary cells and calculated dispersion characteristics of polaritons in such system, taking into account modulation of the refractive index.

The structure of the paper is as follows. In Sec. II we derive a general expression for the transfer matrix for the general case of an arbitrary form of the spatial modulation of the dielectric function and angle of propagation and the polarization state of the electromagnetic wave. In particular we obtain the general form of the effective exciton-light coupling parameter and the radiative shift of the exciton frequency, taking into account the spatial inhomogeneity of the dielectric function in the photonic crystal. We show that by choosing an appropriate basis for representing transfer matrices one can significantly simplify the analysis of the band structure and dispersion laws of electromagnetic excitations in the structures under consideration. In Sec. III we illustrate the power of the approach by applying it to a number of examples, some of which deal with already well-studied situations (passive one-dimensional photonic crystals, optical lattices, MQW's with a piecewise spatial dependence of the dielectric function), while the others demonstrate the possibilities of our approach in obtaining results that could not have been obtained by other methods. In particular, we derive the condition of the resonant light-exciton interaction (Bragg resonance) virtually irrespective of a particular form of the spatial distribution of the dielectric function. Also, we obtain the general expression for the width of the stop band in the case of the Bragg resonance and study the dependence of the band structure on the angle of propagation and the polarization of the electromagnetic wave.

II. (a,f) REPRESENTATION OF THE TRANSFER MATRIX

A. Transfer matrix approach in resonant photonic crystals

A propagation of the electromagnetic wave in structures under discussion is governed by the Maxwell equation

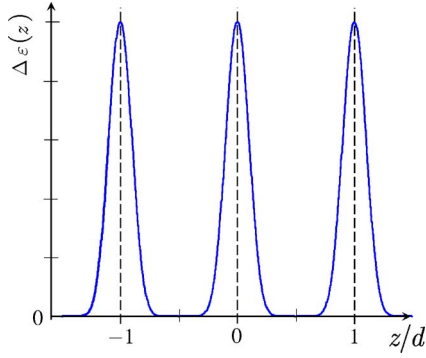


FIG. 1. (Color online) An example of the modulation of the dielectric function, $\epsilon(z) = \bar{\epsilon} + \Delta\epsilon(z)$ (solid line). The dashed vertical lines show the positions of the centers of QW's.

$$\nabla \times \nabla \times \mathbf{E} = \frac{\omega^2}{c^2} [\epsilon_{sc}(z)\mathbf{E} + 4\pi\mathbf{P}_{exc}], \quad (1)$$

where the z axis is chosen along the growth direction and \mathbf{P}_{exc} is the excitonic contribution to the polarization, which can be presented in the following form:

$$\mathbf{P}_{exc} = -\chi(\omega) \sum_m \Phi_m(z) \int dz' \Phi_m(z') \mathbf{E}_\perp(z'), \quad (2)$$

where $\Phi_m(z) = \Phi(z - z_m)$ is the envelope wave function of an exciton localized in the m th QW. The summation in Eq. (2) is performed over all QW's, and z_m are the positions of their centers. We assume that the distance between the consecutive wells, $d = z_{m+1} - z_m$, coincides with the period of the spatial modulation of the dielectric function, $\epsilon(z+d) = \epsilon(z)$. Also, we assume that the profile of the dielectric function is symmetrical with respect to the position of the center of the QW, $\epsilon(z_m + z) = \epsilon(z_m - z)$ (see Fig. 1). We restrict ourselves to the consideration of $1s$ states of heavy-hole excitons and neglect their in-plane dispersion. The dipole moment of these excitons lies in the plane of the well; therefore, they can only interact with the in-plane component of the electric field, \mathbf{E}_\perp . This fact is reflected in Eq. (2), where only this component of the field is included.

The frequency dependence of the excitonic response is given by the function $\chi(\omega)$, defined as

$$\chi(\omega) = \frac{\alpha}{\omega_0 - \omega - i\gamma}, \quad (3)$$

where ω_0 is the exciton resonance frequency, γ is the nonradiative decay rate of the exciton, and α is the microscopic exciton-light coupling parameter, proportional to the dipole moment of the electron-heavy-hole transition.

Equation (1) can be analyzed by presenting the direction of the electric field as a vector sum of two mutually perpendicular polarizations. These so-called s and p polarizations define two possible eigendirections, and accordingly, the respective electric fields satisfy two independent equations, which can be considered separately. These polarizations are defined by the direction of the wave vector in the plane perpendicular to the modulation (growth) direction. Obviously,

in the structures modulated along particular directions, the in-plane wave vector is a conserving quantity.

The absence of an overlap of the exciton wave functions localized in different QW's makes it possible to use the transfer matrix technique for solving Maxwell equations, Eq. (1). The general idea of this technique is to characterize the electric field of the wave with a certain polarization by a two-component column vector $|c(z)\rangle$ whose change along the structure is governed by a 2×2 matrix. The main property of this matrix can be described as following. If $|c(z_1)\rangle$, $|c(z_2)\rangle$, and $|c(z_3)\rangle$ characterize the field at points z_1 , z_2 , and z_3 , respectively, and if $\hat{T}(z_i, z_j)$ satisfies the equation $|c(z_i)\rangle = \hat{T}(z_i, z_j)|c(z_j)\rangle$, then $\hat{T}(z_1, z_3) = \hat{T}(z_1, z_2)\hat{T}(z_2, z_3)$. The relations between the values of the field and the vector $|c(z)\rangle$ as well as the form of the matrix $\hat{T}(z_i, z_j)$ depend on the choice of the particular representation of the field. Several possible representations will be discussed in the subsequent sections of the paper for both polarizations.

1. s polarization

In the s -polarized wave the electric field \mathbf{E} is perpendicular to the plane formed by the direction of z axis and in-plane wave vector, \mathbf{k} . Accordingly, it can be presented in the form

$$\mathbf{E}(z, \boldsymbol{\rho}) = \hat{\mathbf{e}}_s E(z) e^{i\mathbf{k}\boldsymbol{\rho}}, \quad (4)$$

where $\boldsymbol{\rho}$ is the coordinate in the (x, y) plane and $\hat{\mathbf{e}}_s = \hat{\mathbf{e}}_k \times \hat{\mathbf{e}}_z$ is a unit polarization vector, defined in terms of unit vectors in the z and \mathbf{k} directions. For $E(z)$ we obtain an integro-differential equation

$$\frac{d^2 E(z)}{dz^2} + \kappa_s^2(z) E(z) = -\chi(\omega) \frac{4\pi\omega^2}{c^2} \sum_m \Phi_m(z) \int dz' \Phi_m(z') E(z'), \quad (5)$$

where $\kappa_s^2(z) = \omega^2 \epsilon(z) / c^2 - k^2$.

We first consider the transfer matrix corresponding to the propagation of the field across one elementary cell of the structure—i.e., from point $z_- + 0$ at the left boundary of the cell, inside it, to the point $z_+ + 0$ just outside of the right boundary of the cell. The complete transfer matrix connecting the field at the right boundary of the entire system with the field at its left boundary can then be obtained as a product of the transfer matrices for each cell. Considering only one cell, we can, without any loss of generality, choose the origin of our coordinate system coinciding with a position of the QW in the cell under consideration. When z coordinate is confined to a single cell, the summation over QW's and the index enumerating them in Eq. (5) can be dropped.

The term with the exciton polarization on the right-hand side of Eq. (5) can be considered as an inhomogeneity in a second-order differential equation

$$\frac{d^2 E(z)}{dz^2} + \kappa_s^2(z) E(z) = \mathcal{F}(z), \quad (6)$$

whose general solution can be written in the form²⁴

$$E(z) = c_1 h_1(z) + c_2 h_2(z) + (G \star \mathcal{F})(z), \quad (7)$$

where

$$(G \star \mathcal{F})(z) = \int_{z_-}^z dz' \mathcal{F}(z') \frac{h_1(z')h_2(z) - h_1(z)h_2(z')}{W(h_1, h_2; z')}. \quad (8)$$

Here we have introduced $h_{1,2}(z)$, a pair of linearly independent solutions of the homogeneous equation

$$\frac{d^2 E(z)}{dz^2} + \kappa_s^2(z)E = 0, \quad (9)$$

and $W(h_1, h_2; z) = h_1 h_2' - h_1' h_2$ is the Wronskian of these solutions. For the case under consideration the Wronskian does not depend on z and will be denoted by W_h in what follows.

Alternatively, a solution of Eq. (5) can be presented as²⁵

$$\begin{aligned} E(z) &= c_1(z)h_1(z) + c_2(z)h_2(z), \\ E'(z) &= c_1(z)h_1'(z) + c_2(z)h_2'(z). \end{aligned} \quad (10)$$

In the regions outside of the QW, where $\Phi(z) \equiv 0$, the functions $c(z)$ remain constants, but they change when z traverses from one boundary of the QW to the other. Our goal now is to use Eq. (7) along with Eq. (8) in order to relate the values of $c_i(z)$ at the right boundary of the QW to their values at the left boundary. Using these equations we can obtain the expression for the electric field for points to the right from the QW as

$$\begin{aligned} E(z) &= h_1 \left[c_1 + \tilde{\chi} \frac{4\pi\omega^2\varphi_2}{c^2} (c_1\varphi_1 + c_2\varphi_2) \right] \\ &+ h_2 \left[c_2 - \tilde{\chi} \frac{4\pi\omega^2\varphi_1}{c^2} (c_1\varphi_1 + c_2\varphi_2) \right], \end{aligned} \quad (11)$$

where $\varphi_{1,2}$ are ‘‘projections’’ of the solutions $h_{1,2}$ onto the exciton state,

$$\varphi_{1,2} = \frac{1}{W_h} \int_{QW} dz' \Phi(z') h_{1,2}(z'), \quad (12)$$

and the modified excitonic response function $\tilde{\chi}$ can be presented as

$$\tilde{\chi} = \frac{1}{\chi^{-1} - \Delta\omega/\alpha}, \quad (13)$$

where

$$\Delta\omega = \alpha \int_{QW} dz \Phi(z) (G \star \Phi)(z) \quad (14)$$

gives the radiative shift of the exciton frequency in the photonic crystal. Equation (14) is a generalization of the well-known expression for the radiative shift in MQW structures with a homogeneous dielectric function.^{11,26,27}

Comparing Eq. (11) with Eq. (10) and taking into account that the coefficients c_i do not change outside of the QW, we can find a relation between the coefficients c_i determined at the two *inner* boundaries of the elementary cell, $z = z_- + 0$, and $z = z_+ - 0$,

$$\begin{pmatrix} c_1 \\ c_2 \end{pmatrix} (z_+ - 0) = T_h \begin{pmatrix} c_1 \\ c_2 \end{pmatrix} (z_- + 0), \quad (15)$$

with the matrix T_h given as

$$T_h = \mathbf{1} + \frac{4\pi\omega^2\tilde{\chi}}{c^2} \begin{pmatrix} \varphi_2\varphi_1 & \varphi_2^2 \\ -\varphi_1^2 & -\varphi_2\varphi_1 \end{pmatrix}, \quad (16)$$

where $\mathbf{1}$ is the unit matrix. It should be noted that Eq. (16) is valid for an arbitrary form of the exciton envelope wave function and spatial modulation of the dielectric function.

Equation (16) can be significantly simplified if we use freedom in the choice of the functions $h_i(z)$. It follows from the observation that one of $\varphi_{1,2}$ can always be turned to zero by a special choice of the solutions.⁵¹ For example, in the case when $\epsilon(z)$ is invariant with respect to the mirror reflection relatively to the center of the QW, $h_{1,2}$ can be chosen to have a definite parity, with one of them being even with respect to the center of the QW and the other being odd. It should be understood, however, that h_1 and h_2 are not necessarily actual normal modes of the photonic crystal. The latter must be defined as solutions of the appropriate boundary problem and do not have to be even or odd functions with respect to the center of the elementary cell. Moreover, due to the Bloch theorem, the modes of a photonic crystal can have a definite parity only at specific frequencies that are naturally identified with boundaries of the forbidden gap in the spectrum. However, all normal modes of the photonic crystal can be represented as superpositions of the even and odd solutions $h_{1,2}$. A formal discussion of the relation between the functions h_1 and h_2 and the normal modes can be found in Ref. 28 where a similar approach has been used for the analysis of the spectral properties of a Schrödinger equation with a periodic potential.

Obviously, fixing the parity of the solutions does not determine functions h_1 and h_2 uniquely since a multiplication by a constant does not change their symmetry. It can be shown, however, that the results obtained for observable quantities, such as band structure, do not depend on this ambiguity. We will present our general results in a form independent of the choice of initial conditions specified at the center of the elementary cell. However, for discussions of particular examples it is more convenient to fix them in the form

$$h_1(0) = 1, \quad h_1'(0) = 0, \quad h_2(0) = 0, \quad h_2'(0) = 1, \quad (17)$$

for which $W_h = 1$.

Let us assume that h_1 is the even solution; then, $\varphi_2 \equiv 0$ and the expression for the matrix T_h simplifies to

$$T_h = \mathbf{1} + S_s q_s \begin{pmatrix} 0 & 0 \\ 1 & 0 \end{pmatrix}, \quad (18)$$

where $q_s = \kappa_s(z_+)$ is the value of $\kappa_s(z)$ at the boundary of the elementary cell and

$$S_s = -\tilde{\chi}(\omega) \frac{2\pi\omega^2\varphi_1^2}{q_s c^2 W_h}. \quad (19)$$

Substitution of $\tilde{\chi}$ yields

$$S_s = \frac{\Gamma_s}{\omega - \omega_0 - \Delta\omega + i\gamma}, \quad (20)$$

where Γ_s is the radiative decay rate,

$$\Gamma_s = \frac{2\pi\alpha\omega^2\varphi_1^2}{q_s c^2}. \quad (21)$$

The function $S_s(\omega)$, which we shall refer to as exciton susceptibility, describes the contribution of the exciton-light interaction to the optical properties of the structures under consideration. For instance, the resonant absorption of light occurs at the frequency $\tilde{\omega}_0 = \omega_0 + \Delta\omega$ determined by the pole of $S_s(\omega)$. We will treat $\tilde{\omega}_0$ as an experimentally accessible exciton frequency, which along with the radiative decay rate Γ_s can be measured in optical experiments with a single QW. In what follows we will drop the tilde from ω_0 and assume that the radiative shift is included in this parameter.

The coefficients c_i in Eq. (15) are the two components of the vector $|c\rangle$ characterizing the field in the transfer matrix formalism while the matrix T_h given by Eq. (16) is the transfer matrix itself. The functions $h_i(z)$, which we used to derive Eqs. (15) and (18), form a basis for this particular representation of the transfer matrix. Using this basis we are able to obtain a simple and convenient expression for the transfer matrix describing the evolution of the electric field *inside* a single elementary cell. However, in order to obtain the transfer matrix through a period of the structure, we have to relate the field and its derivative at points to the left ($z_+ - 0$) and to the right ($z_+ + 0$) of the boundary between two elementary cells. These relationships can be found by comparing functions $h_i(z)$ defined in different elementary cells. For two adjacent m th and $(m+1)$ th cells, the respective functions $h_i^m(z)$ and $h_i^{m+1}(z)$ are related to each other as $h_i^m(z) = h_i^{m+1}(z-d)$, and in order to establish a connection between the vectors the $|c^m\rangle$ and $|c^{m+1}\rangle$ at the boundary between these cells, one would need to express $h_i^{m+1}(z)$ in the basis of $h_i^m(z)$. This problem can be solved, but it turns out to be more convenient to convert our transfer matrices to a more conventional basis of plane waves,

$$E(z) = E_+ e^{iq_s z} + E_- e^{-iq_s z}, \quad (22)$$

using the conversion rule, Eq. (A9), derived in the Appendix. The resulting transfer matrix describing the evolution of the field across an entire elementary cell can then be presented in the form

$$T = \begin{pmatrix} af & (\bar{a}f - a\bar{f})/2 \\ (a\bar{f} - f\bar{a})/2 & \bar{a}\bar{f} \end{pmatrix}, \quad (23)$$

which, as will be seen shortly, is particularly convenient for analysis of the spectrum of the system under consideration. This representation is extensively used in the present paper and, in what follows, we will refer to it as the (a, f) representation. The parameters of this representation, a and f , are defined as

$$a = g_2, \quad f = g_1 - iS_s g_2,$$

$$\bar{a} = g_2^*, \quad \bar{f} = g_1^* + iS_s g_2^*, \quad (24)$$

where

$$g_1 = \frac{1}{\sqrt{W_h}} \left[h_1(z_+) + \frac{h_1'(z_+)}{iq_s} \right],$$

$$g_2 = \frac{1}{\sqrt{W_h}} [iq_s h_2(z_+) + h_2'(z_+)]. \quad (25)$$

2. *p* polarization

A representation similar to Eq. (23) for a transfer matrix describing *p*-polarized light can also be obtained along similar lines. An important difference is that the electric field in the *p*-polarized waves is not transverse ($\nabla \cdot \mathbf{E} \neq 0$) and, therefore, satisfies a different differential equation. For conventional photonic crystals the *p*-polarized waves are conveniently described in terms of the magnetic field (see, e.g., Ref. 3). However, the presence of the dipole-active excitations significantly reduces the convenience of this approach because in order to close the equation for this field, one would have to express the interaction with excitons in terms of the magnetic field. While it can be done, we find it more convenient to continue working with the electric field \mathbf{E} .

The electric field for the *p* polarization can be presented in the following form:

$$\mathbf{E}(z, \boldsymbol{\rho}) = [\hat{\mathbf{e}}_x E_x(z) + \hat{\mathbf{e}}_z E_z(z)] e^{i\mathbf{k}\boldsymbol{\rho}}. \quad (26)$$

The amplitudes $E_{x,z}(z)$ satisfy the system of equations

$$\frac{d^2 E_x}{dz^2} - ik \frac{dE_z}{dz} + \kappa_p^2(z) E_x$$

$$= -\chi(\omega) \sum_m \Phi_m(z) \int dz' \Phi_m(z') E_x(z'),$$

$$-ik \frac{dE_x}{dz} + [\kappa_p^2(z) - k^2] E_z(z) = 0, \quad (27)$$

where $\kappa_p^2(z) = \omega^2 \epsilon(z) / c^2$. Deriving these equations we again have explicitly taken into account that only the in-plane component of the electric field interacts with the heavy-hole excitons. Solving the second equation with respect to E_z we obtain the closed equation for $E_x(z)$:

$$\frac{d}{dz} \left[p(z) \frac{dE_x}{dz} \right] + \kappa_p^2(z) E_x$$

$$= -\chi(\omega) \frac{4\pi\omega^2}{c^2} \sum_m \Phi_m(z) \int dz' \Phi_m(z') E_x(z'), \quad (28)$$

where $p(z) = \kappa_p^2(z) / [\kappa_p^2(z) - k^2]$. This function is related to the local angle of propagation of the wave, $\theta(z)$: $p(z) = 1 / \cos \theta(z)$.

The derivation of the transfer matrix for the *p*-polarized field follows exactly the same steps as in the previous subsection with one important change. The Wronskian of two solutions of the “homogeneous” (that is, with $\chi \equiv 0$) version

of Eq. (28) depends on the coordinate z .²⁴ This, however, does not present a major problem, because if one takes into account that this dependence can be presented in the form

$$W(z) = W_h \frac{p(z_+)}{p(z)}, \quad (29)$$

one can immediately reproduce all the main results of the previous subsection. In particular, the transfer matrix in the basis of plane waves can again be written down in the (a, f) representation, Eq. (23). The parameters of this representation are given by the same Eqs. (24) and (25), where, however, one has to consider the functions $h_{1,2}$ as even and odd solutions of the “homogeneous” version of Eq. (28). Also, the function S_p , which retains the same form as in Eq. (20), is now characterized by a modified radiative shift of the exciton frequency and the decay rate. The expression for the frequency shift is obtained by replacing the expression given by Eq. (8) with

$$(G \star \mathcal{F})(z) = \frac{1}{W_h p(z_+)} \int_{z_-}^z dz' \mathcal{F}(z') [h_1(z') h_2(z) - h_1(z) h_2(z')] \quad (30)$$

in Eq. (14) for the radiative shift. The rate of exciton’s decay into the p -polarized light is given by

$$\Gamma_p = \frac{2\pi\alpha\omega^2\varphi_1^2}{q_p c^2 p(z_+)}, \quad (31)$$

where $q_p = \kappa_p(z_+)$. One can notice that these expressions and the corresponding expressions for the s -polarized wave coincide in the case of normal propagation—i.e., when $k=0$.

B. General properties of the (a, f) representation

The fact that the transfer matrices for both polarizations allow for the (a, f) representation is not a coincidence but is related to a well-known feature of the Maxwell equations. To demonstrate it let us consider Eq. (28) in a particular case corresponding to the passive structure ($\chi \equiv 0$). If $E(z)$ is a solution to this equation, its complex conjugate $E^*(z)$ is also a solution. Having this in mind one can show that

$$\frac{d}{dz} [p(z)(EE^{*'} - E'E^*)] = 0. \quad (32)$$

Now, representing the electric field in the form of Eq. (22) we can find that

$$\frac{d}{dz} [q_p p(z)(|E_+|^2 - |E_-|^2)] = 0. \quad (33)$$

This relation expresses conservation of the flux of the Poynting vector through a plane perpendicular to the z axis and represents the fact that there are no sources or drains of the energy in the system. The similar expression for the s -polarized wave can be obtained by substitution $q_p \rightarrow q_s$, $p(z) \rightarrow 1$. It follows from Eq. (33) that the transfer matrices through the period for both s and p polarizations must preserve the combination $|E_+|^2 - |E_-|^2$, which means that the

transfer matrix written in the basis of plane waves belongs to the $SU(1,1)$ group.²⁹ A general form of an element of this group is²⁹

$$T = \begin{pmatrix} T_1 & T_2 \\ T_2^* & T_1^* \end{pmatrix}, \quad (34)$$

where $T_{1,2}$ are complex numbers and $|T_1|^2 - |T_2|^2 = 1$. Matrices allowing for the (a, f) representation correspond to a particular case of $SU(1,1)$ matrices, for which T_2 is purely imaginary. It can be shown that such matrices describe structures that possess a mirror symmetry. Indeed, a transfer matrix of such a structure satisfies the condition $\sigma_x T \sigma_x = T^{-1}$, where σ_x is the Pauli matrix. Substitution of Eq. (34) into this equation gives $T_2^* = -T_2$. The converse statement can also be verified. This property of transfer matrices can also be proven in the general case of matrices corresponding to the Maxwell equations (5) and (28) with the external polarization, but the proof is rather technical and we do not provide it here.

Owing to the (a, f) representation, the description of structures with mirror symmetry can be significantly simplified. At the same time, they demonstrate a rich variety of interesting phenomena and, therefore, these structures have attracted a great deal of attention (see, e.g., Ref. 30). If such a structure is built of blocks that have mirror symmetry by themselves, then the transfer matrix through the entire structure can be written in terms of matrix elements describing the individual blocks. Indeed, let us consider a structure with period BAB where the transfer matrices of blocks A and B have the form $T(a_1, f_1)$ and $T(a_2, f_2)$, respectively, in the (a, f) representation. Then it can be shown that the transfer matrix through the period is

$$T(a_2, f_2) T(a_1, f_1) T(a_2, f_2) = T(a, f), \quad (35)$$

where

$$a = a_1 a_2 f_2 - \frac{\bar{a}_1}{2} (\bar{a}_2 f_2 - a_2 \bar{f}_2),$$

$$f = f_2 f_1 a_2 + \frac{\bar{f}_1}{2} (\bar{a}_2 f_2 - a_2 \bar{f}_2). \quad (36)$$

We will illustrate the “multiplication rule,” Eq. (35), considering a simple but very important for the rest of the paper example of an elementary cell in an optical lattice. In this system, block A corresponds to an active element—for instance, a QW—and two blocks B describe barriers, which have the *same* refractive index as block A . Blocks B are described by a transfer matrix given by $T_b(\phi_b) = \text{diag}[\exp(i\phi_b), \exp(-i\phi_b)]$. In this case one has $a_2 = f_2 = \exp(i\phi_b/2)$ in Eq. (35) and thus

$$T_b(\phi_b) T(a, f) T_b(\phi_b) = T(ae^{i\phi_b}, fe^{i\phi_b}). \quad (37)$$

If, however, one needs to take into account the difference between refractive indices of blocks B and block A , a type of transfer matrix product emerges. Introducing matrix T_ρ , describing propagation of light across a boundary between two media with different indexes of refraction

$$T_\rho = \frac{1}{1+\rho} \begin{pmatrix} 1 & \rho \\ \rho & 1 \end{pmatrix}, \quad (38)$$

where ρ is the Fresnel reflection coefficient³¹ [see below Eq. (49)], we can describe propagation of light through BA and AB interfaces and across block A using the following combination of the transfer matrices: $T_\rho(\rho)^{-1}T(a,f)T_\rho(\rho)$. An important property of the (a,f) representation is that this product can be expressed in the following form:

$$T_\rho(\rho)^{-1}T(a,f)T_\rho(\rho) = \frac{1}{1-\rho^2}T(a+\bar{a}\rho, f-\bar{f}\rho). \quad (39)$$

The real factor in Eq. (39) can be incorporated into a and f due to the useful relation (with real λ)

$$\lambda T(a,f) = T(\lambda a, f) = T(a, \lambda f). \quad (40)$$

Equations (35), (37), and (39) will be extensively used throughout the paper for obtaining the (a,f) representation of various transfer matrices. This method is often more practical than solving corresponding differential equations. Thereby, it is interesting to note that the parameters of the (a,f) representation are essentially boundary values of solutions of the corresponding Cauchy problem. This fact makes it convenient to use the transfer matrix, for example, to relate solutions of a Schrödinger equation with a complex potential and the solutions of simpler problems.

III. DISPERSION EQUATION IN RESONANT PHOTONIC CRYSTALS: THE METHOD OF ANALYSIS AND THE BAND STRUCTURE

A. Dispersion equation in the (a,f) representation

The dispersion equation characterizing normal modes (polaritons) in an infinite periodic one-dimensional structure can be expressed in terms of elements of a transfer matrix across one period of the structure:³²

$$\cos Kd = \frac{1}{2}\text{Tr}T, \quad (41)$$

where K is the Bloch wave number, d is the period of the structure, and the transfer matrix is assumed to be written in the plane-wave basis. If this structure possesses a mirror symmetry, one can show that the condition $\det T=1$ can be presented as $f\bar{a}+\bar{f}a=2$. Using this identity we can rewrite the polariton dispersion law in the form

$$\cos^2\left(\frac{Kd}{2}\right) = \Re(a)\Re(f), \quad (42)$$

where

$$\Re(a) = (a + \bar{a})/2. \quad (43)$$

Equivalently, this dispersion equation can be presented as

$$\sin^2\left(\frac{Kd}{2}\right) = \Im(a)\Im(f), \quad (44)$$

where

$$\Im(a) = (a - \bar{a})/2i. \quad (45)$$

If the exciton susceptibility S is a real function (no homogeneous broadening of excitons), \bar{a} coincides with a conjugated, $\bar{a}=a^*$. In this case, $\Re(a)$ and $\Im(a)$ are equivalent to the regular real or imaginary parts of a , respectively: $\Re(a) = \text{Re}(a)$ and $\Im(a) = \text{Im}(a)$. When homogeneous broadening is taken into account, Eq. (42) remains valid, but identification of $\Re(a)$ and $\Im(a)$ with $\text{Re}(a)$ and $\text{Im}(a)$ can no longer be made. In this case, one has to use the definitions given in Eqs. (43) and (45).

If the homogeneous broadening can be neglected, the right-hand sides of Eqs. (42) and (44) are real valued. Therefore, we can analyze the band structure in the vicinity of the exciton resonance using the notion that for allowed bands (real K) these expressions should be positive and less than unity, while for the band gaps (complex K) they should be negative or greater than unity. Thus, there are two types of conditions determining the boundary of the bands. From Eq. (42) we have that the band boundary occurs when either $\Re(a)\Re(f)$ or $\Re(a)\Re(f)-1$ changes sign, and Eq. (44) defines as the boundaries those frequencies at which the change of sign occurs for expressions $\Im(a)\Im(f)$ or $\Im(a)\Im(f)-1$. One can show that these two pairs of conditions are equivalent to each other. More precisely, the expression $\Re(a)\Re(f)$ changes sign at the same frequencies as the expression $\Im(a)\Im(f)-1$. The same is true for the pair $\Re(a)\Re(f)-1$ and $\Im(a)\Im(f)$. Thus, all the band boundaries can be found by considering changes of the sign of the expressions $\Re(a)\Re(f)$ and $\Im(a)\Im(f)$, with negative values corresponding to the band gaps. The factorized form of the right-hand sides of the polariton dispersion equation, Eqs. (42) and (44), drastically simplifies the analysis of the spectrum, as will be seen in the subsequent subsections.

The factorization of the dispersion equations (42) and (44) becomes possible only owing to the (a,f) representation of the transfer matrix, which makes this representation particularly suitable for studying the band structure and dispersion laws of polaritons in resonant photonic crystals. At the same time, this representation is not very convenient for calculating reflection and transmission spectra of finite structures because of a cumbersome relation between the parameters of a single-layer transfer matrix and a matrix describing the entire structure. This problem, however, can be conveniently solved with the help of a different representation introduced in our recent paper, Ref. 23. It is useful to establish a direct relationship between these two representations. First we notice that an arbitrary matrix of the form (23) can be written in the form of a transfer matrix describing propagation of a wave across a single QW [see Eq. (55) below]. This can be done by introducing an effective optical width of one period of the structure, $\tilde{\phi}$, and an effective excitonic susceptibility \tilde{S} . The relation between the parameters of the (a,f) representation and these effective parameters can be found by comparing Eqs. (23) and (55):

$$\tilde{S} = \frac{1}{2i}(a\bar{f} - \bar{a}f), \quad e^{i\tilde{\phi}} = \frac{a}{\bar{a}}. \quad (46)$$

The usefulness of this relation is twofold. First, it shows that for any resonant photonic crystal the transfer matrix through

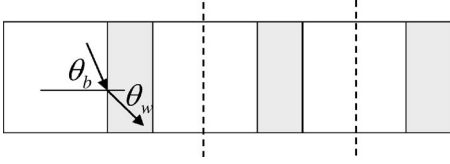


FIG. 2. The periodic structure built of two blocks. Vertical dashed lines show the boundary of the elementary cell. The angles of propagation inside the blocks are related by Snell's law.

the period can be represented as a transfer matrix through a conventional MQW structure. Second, Eq. (46) can be used for a consideration of reflection and transmission spectra of a structure described by a transfer matrix in (a, f) representation. This is where the introduction of \tilde{S} and $\tilde{\phi}$ and then, consecutively, the representation of the transfer matrix in terms of parameters θ and β of Ref. 23 become very convenient. However, this representation misses the possibility to factorize the dispersion equation, so it is not very suitable for a constructive analysis of the dispersion law. One can see, therefore, that the representations of the transfer matrix in terms of parameters (a, f) and \tilde{S} and $\tilde{\phi}$ complement each other in the sense that each of them is suited best for its own set of problems.

B. MQW structures with a simple elementary cell

As was mentioned in the Introduction, MQW structures present one example of RPC's, in which effects due to reflection of light from well-barrier interfaces coexist with effects due to the resonant light-exciton coupling. The spatial profile of the refractive index in these structures is particularly simple and is described by a piecewise constant function (Fig. 2). Various properties of these structures have been studied in a number of publications,^{20,21,23,26,33-35} including Refs. 20 and 21, where the dispersion laws and the band structure were studied in the scalar model for polaritons propagating along the growth direction.

Nevertheless, we find it useful to consider this case in detail in this paper because it gives a clear illustration of using the (a, f) representation for the analysis of complex dispersion equations.

We start by considering two particular cases: a passive photonic crystal (no resonances) and an optical lattice (no refractive index mismatch). This will give us useful benchmarks for discussing the general situation. In the latter case we will neglect the exciton homogeneous broadening, which allows us to identify the operations \mathfrak{R} and \mathfrak{I} by taking the regular real and imaginary parts of the respective expressions. The same is obviously true for the case of passive structures.

1. Passive photonic crystals

Let us consider a structure built of a periodic sequence of two blocks characterized by the widths $d_{b,w}$ and the indices of refraction $n_{b,w}$. To emphasize the mirror symmetry we choose the elementary cell as shown in Fig. 2. The transfer matrix through the period of the structure has the form

$$T = T_b^{1/2} T_p^{-1} T_w T_p T_b^{1/2}, \quad (47)$$

where

$$T_{b,w} = \begin{pmatrix} e^{i\phi_{b,w}} & 0 \\ 0 & e^{-i\phi_{b,w}} \end{pmatrix}, \quad (48)$$

and $\phi_{b,w} = \omega n_{b,w} d_{b,w} \cos \theta_{b,w} / c$ and $\theta_{b,w}$ are the angles of propagation of the wave.

The scattering of the electromagnetic wave at the interface between different blocks depends on both the angle of incidence of the wave and its polarization state. These effects are described by Fresnel coefficients ρ_s and ρ_p ,

$$\rho_s = \frac{n_w \cos \theta_w - n_b \cos \theta_b}{n_w \cos \theta_w + n_b \cos \theta_b},$$

$$\rho_p = \frac{n_w \cos \theta_b - n_b \cos \theta_w}{n_w \cos \theta_b + n_b \cos \theta_w}, \quad (49)$$

for s and p polarizations, respectively. Below we denote the Fresnel coefficients simply by ρ , having in mind that for a particular polarization only one of these expressions should be used.

Using Eqs. (37) and (39) we can find parameters of the (a, f) representation of the transfer matrix, which in this case take the form

$$a = \frac{e^{i\omega\tau_+} + \rho e^{i\omega\tau_-}}{1 - \rho^2}, \quad f = e^{i\omega\tau_+} - \rho e^{i\omega\tau_-}, \quad (50)$$

where $\tau_{\pm} = (\phi_b \pm \phi_w) / 2\omega$. Now we can use general dispersion equations (42) and (44) to analyze the structure of the allowed and forbidden bands of this system. As we discussed in Sec. III A there are two types of forbidden bands, determined by conditions $\text{Re}(a)\text{Re}(f) < 0$ and $\text{Im}(a)\text{Im}(f) < 0$, respectively. If τ_+ and τ_- are incommensurate, these band gaps alternate along the frequency axis and can be classified as either odd (first, third, etc.) or even (second, fourth, etc.).

Since the coefficients of the dispersion equation in the passive photonic crystals do not contain any singularities, its right-hand side can only change the sign by passing through zero. Thus, the band boundaries are situated at the frequencies where either $\text{Re}(a)\text{Re}(f) = 0$ or $\text{Im}(a)\text{Im}(f) = 0$. For instance, if $\rho > 0$, the boundaries of odd band gaps are determined by the equations

$$\text{Re}[a(\Omega_+)] = 0, \quad \text{Re}[f(\Omega_-)] = 0, \quad (51)$$

where Ω_- and Ω_+ correspond to the lower- and higher-frequency boundaries of a given band gap, respectively. The explicit form of these equations can be obtained using the definitions of a and f , Eq. (50):

$$\cos(\Omega_- \tau_+) - \rho \cos(\Omega_- \tau_-) = 0,$$

$$\cos(\Omega_+ \tau_+) + \rho \cos(\Omega_+ \tau_-) = 0. \quad (52)$$

In the simplest case, when the layers have the same optical width, one has $\tau_- = 0$ and the positions of the forbidden gap are $\omega_r [1 \pm 2 \arcsin(\rho) / \pi]$, where

$$\omega_r \tau_+ = \frac{\pi}{2}. \quad (53)$$

While this case gives a convenient reference point, however, having in mind applications to MQW structures, an opposite situation, when the optical widths of the layers are different, is of more interest. Generally, as one can see from Eq. (52), the boundaries of the gap are situated asymmetrically with respect to ω_r . Under the assumption of narrow gaps, which is fulfilled for a not very strong contrast of the refraction indexes and for angles not too close to the angle of the total internal reflection, the positions of the boundaries are given by

$$\Omega_{\pm} = \omega_r \left(1 \pm \frac{2\rho \sin \phi_w}{\pi(1 \pm \rho \cos \phi_w)} \right). \quad (54)$$

2. Semiconductor optical lattice

In this case we assume that all layers in the structure have the same index of refraction, n , but there are dipole active excitations in QW's. The propagation of light through a QW is described by the transfer matrix of the form

$$T_w = \begin{pmatrix} e^{i\phi_w}(1 - iS) & -iS \\ iS & e^{-i\phi_w}(1 + iS) \end{pmatrix}, \quad (55)$$

where $\phi_w = \omega n d_w \cos \theta_w / c$. The parameters of the (a, f) representation of T_w are

$$a = e^{i\phi_w/2}, \quad f = e^{i\phi_w/2}(1 - iS). \quad (56)$$

The excitonic contribution to the scattering of light is described by

$$S = \frac{\Gamma_0}{\omega - \omega_0 + i\gamma}. \quad (57)$$

The radiative decay rate Γ_0 depends on the angle of incidence. As follows from Eqs. (21) and (31), for structures with a homogeneous dielectric function these dependences for different polarizations are^{20,36,37}

$$\Gamma_0^{(s)} = \Gamma_0 / \cos \theta_w, \quad \Gamma_0^{(p)} = \Gamma_0 \cos \theta_w. \quad (58)$$

The transfer matrix through the period of the structure is

$$T = T_b^{1/2} T_w T_b^{1/2}. \quad (59)$$

Taking into account the multiplication rule (37), we can find parameters of the (a, f) representation for the entire matrix (59) and the respective dispersion equation^{6,8,38}

$$\cos^2 \left(\frac{Kd}{2} \right) = \cos \omega \tau_+ (\cos \omega \tau_+ + S \sin \omega \tau_+). \quad (60)$$

Unlike the case of the passive photonic crystal, the coefficients of the (a, f) representation now contain a singularity at the frequency of the exciton resonance (we neglect the homogeneous broadening of the excitons here). Therefore, the right-hand side (RHS) of the dispersion equation (60) can change its sign by passing not only through zero, but also through infinity when ω crosses ω_0 . In the general case the

width of the band gap associated with the exciton resonance is proportional to Γ , which is many orders of magnitude smaller than ω_0 . Therefore, usually, exciton-related modifications of the photon dispersion law in the optical lattice are negligible. This situation changes, however, if we require that this singularity be canceled by the term $\cos(\omega \tau_+)$, which happens if $\cos(\omega_0 \tau_+) = 0$. This is equivalent to the condition for the Bragg resonance, when the half-wavelength of the radiation at the exciton frequency is equal to an odd multiplier of the period of the structure:

$$\omega_0 \tau_+ = \frac{\pi}{2} + \pi n. \quad (61)$$

The spectrum of such structures is characterized by a much wider band gap with the width equal to

$$\Delta_{\Gamma} = 2 \sqrt{\frac{\Gamma_0}{\tau_+}} = 2 \sqrt{\frac{2\Gamma_0 \omega_0}{\pi(1 + 2n)}} \quad (62)$$

and is indicative of enhanced coupling between light and QW excitons.

3. MQW structures with a mismatch of the indices of refraction

Now we are ready to discuss the general case of MQW structures with the contrast of the refractive indices. The transfer matrix for this structure is obtained from Eq. (59) by taking into account the scattering at the interfaces between the QW's and barriers,

$$T = T_b^{1/2} T_{\rho}^{-1} T_w T_{\rho} T_b^{1/2}. \quad (63)$$

The dispersion equation following from the (a, f) representation of this transfer matrix has the form

$$\cos^2 \left(\frac{Kd}{2} \right) = \frac{1}{1 - \rho^2} \operatorname{Re}(a_{PC}) [\operatorname{Re}(f_{PC}) + S \operatorname{Im}(a_{PC})], \quad (64)$$

where a_{PC} and f_{PC} are calculated for a passive multilayer structure and are given by Eqs. (50).

Similarly to the case of the optical lattice, the structure of the spectrum near the exciton frequency is complicated by the singular character of the excitonic susceptibility (see Fig. 3), which gives rise to branches of exciton related collective excitations¹⁵ and respective band gaps. We, however, will again focus on structures characterized by the cancellation of the excitonic singularity. As a result, an anomalously broad band gap in the vicinity of the exciton frequency is formed. As one can see from Eq. (44), such a cancellation occurs when either $\operatorname{Re}[a_{PC}(\omega_0)] = 0$ or $\operatorname{Im}[a_{PC}(\omega_0)] = 0$. Both these cases imply that the exciton frequency coincides with a boundary of one of the photonic band gaps. Most experiments with these systems tend to deal with structures having as short a period as possible. Therefore, we only consider the case when $\omega_0 = \Omega_+$, where Ω_+ is the boundary of the lowest band gap of the respective photonic crystal, determined by the first equation of Eqs. (51). The exciton-related band gap in this case appears at the frequencies where the RHS of Eq. (64) is negative.

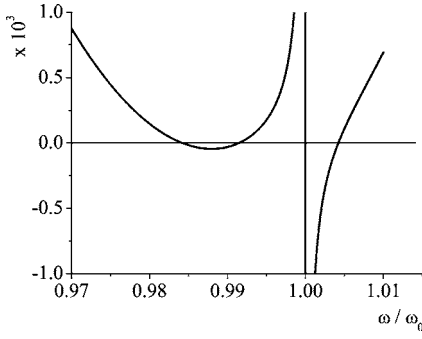


FIG. 3. Plot of the RHS of Eq. (64) scaled by 10^3 for a structure slightly detuned from the Bragg resonance as a function of frequency. The material parameters are chosen to be close to typical parameters of GaAs/Al_xGa_{1-x}As structures: $\rho=0.03$, $\Gamma_0=60 \mu\text{eV}$, and $\omega_0=1.5 \text{ eV}$. The frequencies where this expression is negative or exceeds unity (not shown in this plot) correspond to band gaps. The vertical line shows the position of the exciton frequency.

Assuming a smallness of the gap we can expand a_{PC} and f_{PC} near the frequencies Ω_{\pm} ,

$$\text{Re}[a_{PC}(\omega)] = (\Omega_+ - \omega)t_+, \quad \text{Re}[f_{PC}(\omega)] = (\Omega_- - \omega)t_-, \quad (65)$$

and write the equation for the boundaries of the forbidden gaps in the form

$$(\omega - \Omega_+)(\omega - \Omega_-) - \Gamma_0 \frac{\text{Im}(a_{PC})}{t_-} = 0, \quad (66)$$

where

$$t_+ = \left| \frac{d}{d\omega} \text{Re}[a_{PC}(\omega)] \right|_{\Omega_+}, \quad t_- = \left| \frac{d}{d\omega} \text{Re}[f_{PC}(\omega)] \right|_{\Omega_-}. \quad (67)$$

In Eqs. (65) we explicitly have taken into account the negative sign of these derivatives. In Eq. (66) the radiative decay rate Γ_0 is defined in Eqs. (58) and should be taken according to the polarization of the wave and the angle of propagation.

Using these approximations we can present the boundaries of the polariton band gap as

$$\omega_{\pm} = \Omega_c \pm \frac{1}{2}\Delta, \quad (68)$$

where $\Omega_c = (\Omega_- + \Omega_+)/2$ is the center of the gap and Δ is its width. The expression for Δ can be written in the form

$$\Delta = \sqrt{\Delta_{PC}^2 + \tilde{\Delta}_{\Gamma}^2} \quad (69)$$

and is equal to a ‘‘Pythagorean sum’’ of the widths of the passive photonic gap, $\Delta_{PC} = |\Omega_+ - \Omega_-|$, and the modified excitonic gap,

$$\tilde{\Delta}_{\Gamma}^2 = \Gamma_0 \frac{4 \text{Im}(a_{PC})}{t_-} \approx \Delta_{\Gamma}^2 \frac{1 + \rho}{1 - \rho}. \quad (70)$$

The last formula in this equation is obtained by using the approximate expressions $\text{Im}(a_{PC}) \approx 1 + \rho$ and $t_- \approx \tau_+(1 - \rho)$ which are valid provided that the optical width of the wells is

very small compared to the width of the barriers.

The equation

$$\omega_0 = \Omega_+ \quad (71)$$

generalizes the condition for the Bragg resonance given by Eq. (61) for optical lattices. Indeed, normal modes in photonic crystals are characterized by the Bloch wave number K_{PC} , rather than by the wave number of a homogeneous medium $\omega n/c$. For the band boundaries $\omega = \Omega_{\pm}$ one has $K_{PC}(\Omega_{\pm})d = \pi$, so that $\omega_0 = \Omega_+$ is equivalent to $K_{PC}(\omega_0)d = \pi$, which is a direct generalization of Eq. (61), expressed in terms of the appropriate wave number.

While the results presented have been obtained using the assumption that $\rho > 0$ (that is, for the normal propagation $n_w > n_b$), they remain valid in the opposite case due to the symmetry of the transfer matrix under the transformations $\rho \rightarrow -\rho$ and $a_{PC} \leftrightarrow f_{PC}$. In other words, when we have the opposite relation between n_w and n_b all the arguments used above can be repeated with the mirror reflection of the frequency axis with respect to the center of the photonic gap. In particular, the Bragg resonance occurs when the exciton frequency coincides with the left (low-frequency) edge of the photonic band gap.

4. Angular dependence of the band structure

In previous publications on the band structure of MQW systems²¹ only modes propagating along the growth direction of the structure were considered. In this paper, thanks to the general nature of our approach, we can consider waves propagating at an arbitrary angle treating both s and p polarizations of the electromagnetic waves on equal footing. The foundation for this consideration is laid by the results of the previous subsections, where the expressions for the parameters defining the band structure were derived in terms of Fresnel coefficients, Eqs. (49). The latter contain all the information about the angular and polarization dependences of resonant as well as refractive index contrast contributions to the band structure.

It is clear from Eq. (54) that the Bragg frequency defined by the generalized Bragg condition, Eq. (71), depends on the propagation angle of the wave. This dependence is presented in Fig. 4 for both s - and p -polarized modes. Due to the narrowness of the QW’s, the position of the Bragg resonance approximately follows the renormalization of the optical width of the period of the structure, $\propto \cos(\theta_b)$, for both polarizations. This effect can be used to tune the position of the band gap of the structure. Indeed, if one changes the position of the exciton frequency, by, for instance, using a quantum-confined Stark effect,³⁹ the system can be tuned back to the Bragg resonance by changing the propagation angle of the wave. Assuming that the structure remains tuned to the Bragg condition with the changing angle we can consider the angular dependence of the width of the polariton band gap. One can see from Fig. 4, where this width is presented by vertical bars, that its angular dependence is different for different polarizations. For the s polarization the width monotonously increases when the angle increases, while for the p polarization it, first, decreases, reaches its minimum at Brewster’s angle determined by the equation $\sin \theta_b = n_w / \sqrt{n_w^2 + n_w^2}$

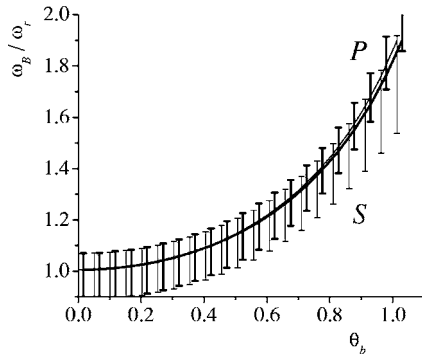


FIG. 4. Dependence of the Bragg resonance frequency ω_B/ω_r [see Eq. (53)] on the angle of propagation θ_b measured in the barriers. The material parameters are the same as in Fig. 3. Bold and thin lines correspond to p and s polarizations, respectively. The vertical lines (the error bars) show the forbidden gap for each polarization. For better visibility the gap is scaled by the factor of 5.

(it corresponds to $\theta_b \approx 0.8$ in Fig. 4), where the only contribution to the gap is due to the exciton-light interaction, and then starts increasing. It should be noted that at Brewster's angle the Fresnel coefficient ρ_p changes its sign. Thus, as has been pointed out above, the condition of the Bragg resonance for the p -polarized wave propagating at angles larger than Brewster's angle is formulated as the equality of the exciton frequency and the lower-frequency edge of the photonic band gap for the p -polarized wave.

Structures with both fixed exciton frequency and period can be tuned to the Bragg resonance at a single angle only. For waves propagating at other angles the Bragg condition is violated and the structure becomes detuned from the resonance. In the case of small detunings, it is natural to refer to such systems as off-Bragg systems. Thus, discussion of the angular dependence of the band structure naturally involves considering the properties of the off-Bragg structures.

When the exciton frequency is not tuned to Ω_+ , one has to take into account the singularity of the exciton susceptibility when looking for the boundaries between allowed and forbidden bands. This singularity results in a narrow band gap situated between zeros of Eq. (44)—i.e., where $\sin^2(Kd/2) < 0$. This band gap occupies the region between ω_0 and $\omega_0 + \Omega_\delta$, where

$$\Omega_\delta = \frac{\pi}{2} \tau_+ \delta \tilde{\Delta}_\Gamma^2 \quad (72)$$

and $\delta = \omega_0 - \Omega_+ \neq 0$. For slightly off-Bragg structures, the width of this addition to the band gap is small, and we will neglect its existence in future discussions. Thus, the band boundaries are determined by zeros of RHS of Eq. (42), and as the result the band structure is determined by four frequencies: ω_0 and the roots of the equation

$$(\omega - \Omega_+) \left[(\omega - \Omega_-)(\omega - \omega_0) - \frac{\tilde{\Delta}_\Gamma^2}{4} \right] = 0. \quad (73)$$

The band structure is characterized by two band gaps and one allowed band between them. If we put these four frequencies in ascending order, the band gaps will lie between

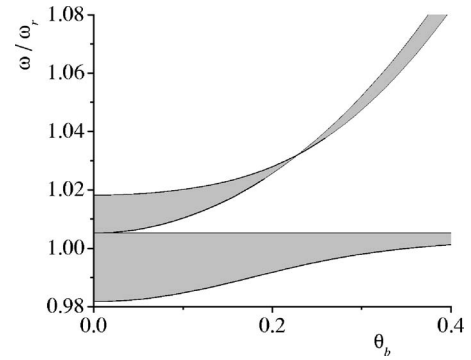


FIG. 5. The dependence of the band gap structure of the s -polarized wave on the angle of propagation θ_b measured in the barriers. The material parameters are the same as in Fig. 3. The dashed regions correspond to the forbidden gaps. The structure is assumed to be tuned to the Bragg resonance at normal propagation.

the first and second pairs of frequencies separated by a transparency window (see Fig. 3). The exact order of the band boundaries depends on relation between ω_0 and Ω_+ . If $\omega_0 < \Omega_+$ then the band gaps are between ω'_- and ω_0 and between Ω_+ and ω'_+ , where

$$\omega'_\pm = \Omega_c + \frac{\delta}{2} \pm \frac{1}{2} \sqrt{(\Delta_{PC} - \delta)^2 + \tilde{\Delta}_\Gamma^2}, \quad (74)$$

while the allowed band is between ω_0 and Ω_+ . Thus, detuning the exciton resonance frequency away from Ω_+ leads to the appearance of a transparency window between ω_0 and Ω_+ inside the band gap obtained for the Bragg case, $\omega_0 = \Omega_+$, and to a slight modification of the external edges of the gap. This result is in a qualitative agreement with the earlier analysis of off-resonant MQW structures.¹⁰ The transparency window would manifest itself in optical spectra as a dip in the reflection coefficient. A similar dip was actually observed in Refs. 9, 23, and 40, where structures with the period satisfying the nonmodified Bragg condition, Eq. (61), were considered. Since the well and barrier materials had different, albeit close, values of the refractive indexes, the real Bragg period should have been determined from Eq. (71) and the structures considered in those papers were actually slightly off-Bragg. It should be mentioned, however, that the detuning from the real Bragg condition could be not the only cause for the observed dip in reflection. The inhomogeneous broadening of the excitons could also contribute to this effect.⁴¹

Now we can describe how the band structure of our system evolves with the changing propagation angle. Let us assume that the system is at the Bragg resonance for the normal incidence. Increasing the angle, we detune it away from the resonance. As a result, two band gaps, one adjacent to the exciton frequency and another detached from it, separated by the transparency window, appear. Figure 5 shows the angular dependence of the band structure for the case of the s polarization. An interesting phenomenon is seen to occur at an angle at which $\Omega_+ = \omega'_+$. In this case, the width of the band gap detached from the exciton frequency turns to zero (band gap collapse). This collapse is a specific feature of RPC's and is absent in both purely passive structures and

optical lattices. An important property of the gap adjacent to ω_0 is its weak polarization dependence. This can be understood if one notices that any difference between polarizations could only appear at angles where $\omega_B - \omega_0 \gg \tilde{\Delta}_\Gamma, \Delta_{PC}$. The width of the adjacent gap for these angles can be found from Eq. (74). It is equal to

$$\Delta_{\text{adj}} \approx \frac{\tilde{\Delta}_\Gamma^2}{\Omega_- - \omega_0}. \quad (75)$$

With the accuracy up to the terms $\sim \Delta_{\text{adj}} \Delta_{PC} / (\omega_B - \omega_0)$, it is the same for both polarizations. The property of omnidirectional reflectivity—i.e., a resonant reflection at all angles of incidence—ensues from these results. It follows from the notion that a usual scattering problem is set up for a structure embedded in a medium with essentially a lower index of refraction (air or vacuum). As the result, the angles of propagation inside the structure cannot exceed the angle of the internal reflection θ_c at the boundary between the structure and surrounding medium. Therefore, for all angles of incidence the range of frequencies between ω_0 and $\omega'_1(\theta_c)$ corresponds to the forbidden gap and, therefore, to a resonant reflection. A similar effect has been considered for the case of passive photonic crystals in a number of publications.^{42–45} Here we want to emphasize the feature specific for the RPC. If the angle of total internal reflection is small (for the air-GaAs interface $\theta_c \approx 0.28$), we can describe the change of the edges of the photonic band gap by a simple renormalization of the optical width of the period, $\Omega_\pm \rightarrow \Omega_\pm / \cos \theta$. It results in the width of the region corresponding to omnidirectional reflection in the form

$$\Delta_{\text{omni}} \approx \frac{1}{2} \frac{\tilde{\Delta}_\Gamma^2}{\Omega_+ \sin^2 \theta_c - 2\Delta_{PC}}, \quad (76)$$

where we have assumed that the photonic forbidden gap is not too wide—i.e., $\Omega_+ \sin^2 \theta_c > 2\Delta_{PC}$. One can see that the presence of QW's essentially weakens the condition of the omnidirectionality in comparison with passive photonic crystals.

C. General modulation of the dielectric function

1. Resonant photonic crystals

The formalism developed in this paper allows us to analyze the band structure in RPC's with an arbitrary periodic modulation of the dielectric function. Using the (a, f) representation for transfer matrices and expressions for the parameters a and f given by Eqs. (24), we can derive the dispersion equation for such a structure in the form similar to Eq. (42),

$$\cos^2\left(\frac{Kd}{2}\right) = \frac{h'_2(z_+)}{W_h} [h_1(z_+) + Sqh_2(z_+)], \quad (77)$$

or Eq. (44),

$$\sin^2\left(\frac{Kd}{2}\right) = -\frac{h_2(z_+)}{W_h} [h'_1(z_+) + Sqh'_2(z_+)]. \quad (78)$$

These dispersion equations can be used to describe waves of all polarizations by choosing the parameters appropriate for a

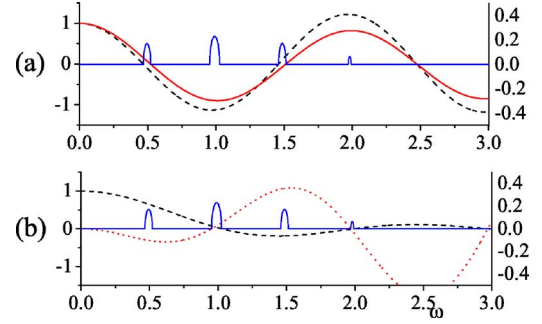


FIG. 6. (Color online) Dependence of $\text{Im}(Kd)$ (solid lines, left axes) and the boundary values of the solutions of the homogeneous Maxwell equations and their derivatives (dashed and dotted lines, respectively, right axes) on the frequency for a passive structure ($S \equiv 0$). The nonzero values of $\text{Im}(Kd)$ correspond to the band gaps. The index of refraction is $n(z) = 3 + \cos^{20}(\pi z/2)$. (a) Kd is the solution of Eq. (77), $h_1(\omega)$, and the dotted line depicts $h'_2(\omega)$. (b) Kd has been found from Eq. (78), the dashed line represents $h_2(\omega)$, and the dotted line depicts $h'_1(\omega)/5$. One can see how zeros of the boundary values determine consecutive band boundaries.

given polarization, S , q , and $h_{1,2}$. The band structure of a passive photonic crystal can be obtained from these equations by setting $\chi \equiv 0$. The band boundaries Ω_\pm in this case are determined by the equations

$$h_1(z_+, \Omega_-) = 0, \quad h'_2(z_+, \Omega_+) = 0 \quad (79)$$

and

$$h'_1(z_+, \Omega_-) = 0, \quad h_2(z_+, \Omega_+) = 0, \quad (80)$$

where Ω_\mp in the argument denote that the functions $h_{1,2}$ are solutions of corresponding homogeneous equations [Eq. (5) or (28) with $\chi \equiv 0$] for $\omega = \Omega_\mp$ respectively. Thus the zeros of even and the maxima of odd solutions given by Eqs. (79) and (80) determine the boundaries of the consecutive band gaps in the band structure of the system under consideration (see Fig. 6).

The analysis of the full dispersion equations, with the resonance terms restored, repeats the analysis of the previous subsection, where one needs to make the substitutions $a_{PC} = g_2$ and $f_{PC} = g_1$. In particular, the parameters t_\pm of the equation for the boundaries of the forbidden gap, Eq. (66), are defined in terms of boundary values of $f_{1,2}$ as

$$t_- = \frac{1}{\sqrt{W_h}} \left| \frac{\partial h_1(\Omega_-)}{\partial \omega} \right|, \quad t_+ = \frac{1}{\sqrt{W_h}} \left| \frac{\partial h'_2(\Omega_+)}{\partial \omega} \right|. \quad (81)$$

The general structure of the spectrum is similar to the one discussed in the case of the piecewise modulation of the refractive index, and we can generalize the condition for the Bragg resonance, when the exciton-related allowed band collapses, and the spectrum of our system in the vicinity of the exciton frequency consists of a single wide band gap. We again require that the singularity of the excitonic susceptibility at ω_0 be canceled by the first term $h'_2(z_+)$ in Eq. (77). This corresponds to the condition $\omega_0 = \Omega_+$, where Ω_+ is the high-frequency boundary of the respective photonic gap. From the dispersion equation (79) it follows again that the Bragg con-

dition can be cast in the form $K_{PC}(\omega_0)d=\pi$. For practical calculations the Bragg condition can be conveniently rewritten in the form which does not refer to a solution of the photonic dispersion equation. At the point where $h'_2=0$ one finds that $a/\bar{a}=-1$, yielding $\tilde{\phi}(\Omega_+)=\pi$ [see Eq. (46)]. Thus, the Bragg condition becomes $\tilde{\phi}(\omega_0)=\pi$.

We can also generalize the expression for the width of the band gap in the case of the Bragg resonance. Performing the expansion similar to Eqs. (65) we can obtain the equation for boundaries of the forbidden gap:

$$(\omega - \Omega_+) \left(\omega - \Omega_- - \frac{\tilde{\Delta}_\Gamma^2/4}{\omega - \omega_0} \right) = 0, \quad (82)$$

with $\tilde{\Delta}_\Gamma^2$ given by the first part of Eq. (70). The analysis of Eq. (82) completely repeats that of Eq. (66). In particular, the width of the forbidden gap is determined by the Pythagorean sum of the photonic and excitonic contributions,

$$\Delta^2 = \Delta_{PC}^2 + \tilde{\Delta}_\Gamma^2, \quad (83)$$

where $\Delta_{PC}=|\Omega_+-\Omega_-|$, and the expression for the excitonic contribution, $\tilde{\Delta}_\Gamma$, can be presented as

$$\left(\frac{\tilde{\Delta}_\Gamma}{\Delta_\Gamma} \right)^2 = \frac{\pi c^2 q_s}{4\Omega_- \omega_0 u_s^{(1)}} \quad \text{and} \quad \left(\frac{\tilde{\Delta}_\Gamma}{\Delta_\Gamma} \right)^2 = \frac{\pi c^2 q_p p(z_+)}{4\Omega_- \omega_0 u_p^{(1)}} \quad (84)$$

for s and p polarizations, respectively. Here we have introduced

$$u_{s,p}^{(1)} = \frac{1}{2} \int dz \epsilon(z) \mathbf{E}_{s,p}^{(1)2}, \quad (85)$$

where $\mathbf{E}_{s,p}^{(1)}$ are the s - and p -polarized electric fields corresponding to the even mode of the photonic crystal. This expression represents the energy associated with the even mode of the photonic crystal concentrated in a single elementary cell.

2. Off-Bragg structures

Our analysis so far has been limited to consideration of the band boundaries and the properties of the band gaps in the resonant photonic crystals. To complete the consideration of the normal modes in these structures we need to discuss solutions of Eqs. (79) and (80) in the allowed bands of the spectrum. These solutions determine the dispersion laws $\omega(K)$ of the photonic crystal polaritons. In the case of Bragg structures and for frequencies in the vicinity of the band edges, the dispersion laws can be presented in the following form:

$$\omega_\pm(K) = \Omega_c \pm \frac{1}{2} \sqrt{\Delta^2 + \zeta^2 (K - K_B)^2}, \quad (86)$$

where $K_B = \pi/d$ is the Bloch wave number corresponding to the boundary of the first Brillouin zone and $\zeta = d/t_+ t_-$. These two branches with positive and negative masses, $m_\pm = \pm 2\hbar^2 \Delta / \zeta^2$, lie in the bands that are above and below the

forbidden gap, respectively. In addition to these branches there is one more dispersionless branch at the exciton frequency $\omega_B(K) = \omega_0$.

For the systems detuned from the exact Bragg resonance, the positions of the band boundaries and properties of the band gaps can be determined by repeating the arguments from the previous subsection; we do not reproduce it here. We however complement that analysis by considering modifications of the dispersion laws of the polariton branches for the off-Bragg structures. If the detuning is not too large, $|\delta| = |\omega_0 - \Omega_+| \lesssim \tilde{\Delta}_\Gamma$, the dispersion laws of the original (present in the Bragg structure) upper and lower polariton branches near the band edges can be written in the form

$$\omega_\pm(K) = \omega'_\pm + \hbar^2 (K - K_B)^2 / 2m_\pm, \quad (87)$$

where ω'_\pm are given by Eq. (74) with the parameters defined by the generalized equations (79), (82), and (84). The renormalized mass parameters m_\pm are defined as

$$m_\pm(\delta) = m_\pm \left(1 - \frac{\Delta_{PC} \delta}{\Delta^2} \pm \frac{2\delta}{\Delta \mp \Delta_{PC}} \right). \quad (88)$$

Comparing this result with Eq. (86) one can notice that detuning from the Bragg resonance results in two main modifications of the dispersion laws: first, the position of the band boundaries have changed and, second, the magnitudes of the masses of the upper and lower polariton branches are no longer equal to each other.

The most dramatic changes occur, however, with the third, originally dispersionless branch. In off-Bragg structures this branch acquires dispersion, which, of course, agrees with the opening of the allowed band in the vicinity of the exciton frequency. The dispersion law characterizing this band for $(K - K_B)/K_B \ll 1$ is given by

$$\omega_B(K) = \Omega_+ + \frac{\zeta^2 \delta}{\tilde{\Delta}_\Gamma^2} (K - K_B)^2. \quad (89)$$

This branch corresponds to excitations dubbed ‘‘Braggaritons’’ in Ref. 15. The mass of this mode, given by $m_B = \tilde{\Delta}_\Gamma^2 / 2\zeta\delta$, is very sensitive to the amount of detuning from the Bragg condition and can be effectively controlled, for instance, by the electric field via the quantum-confined Stark effect. This property of the ‘‘Braggariton’’ branch invited the proposal to use it for slowing, stopping, and storing light in Bragg MQW structures.^{46,47}

3. Homogeneous broadening

We finish our consideration of dispersion properties of RPC's with an arbitrary periodic distribution of the refractive index by discussing effects due to the exciton homogeneous broadening. In the presence of dissipation the concept of band gaps becomes ill defined because the imaginary part of the Bloch wave number, generally speaking, is not zero at all frequencies. Nevertheless, the properties of this imaginary part are of great interest, since they determine the spectral and transport properties of the structures under consideration in the vicinity of what would have been band boundaries in the absence of dissipation. In order to access these properties

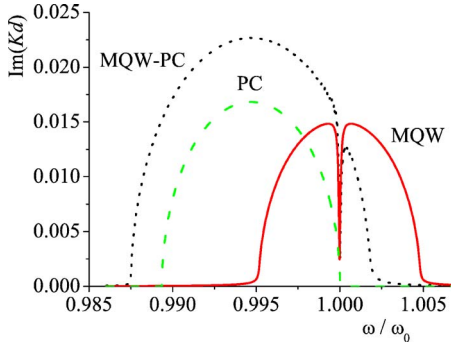


FIG. 7. (Color online) Dependence of $\text{Im}(Kd)$ on frequency for different structures in the vicinity of the first forbidden gap when the exciton homogeneous broadening is taken into account. The dashed line represents the passive structure from Fig. 6. The solid line shows a Bragg MQW structure with a homogeneous dielectric function. The dotted line represents the structure with combination of QW's and the smooth modulation of the dielectric function. The characteristic feature is a divergence of the penetration length $(\text{Im } K)^{-1}$ at the exciton frequency.

we have to consider solutions of Eq. (77). Taking into account that in the spectral region of interest the real part of K is close to π/d , we look for solutions to this equation in the form

$$Kd = \pi + i\lambda. \quad (90)$$

The unknown parameter λ here has a simple physical meaning: the inverse of its real part determines a characteristic length on which the amplitude of the mode decays. The same length determines the penetration depth of incident radiation; therefore, it is often called a penetration length. Assuming that λ is small we can find an approximate expression for it in the form

$$\lambda^2 = 4t_+t_-(\Omega_+ - \omega) \left(\omega - \Omega_- - \frac{\tilde{\Delta}_\Gamma^2/4}{\omega - \omega_0 - i\gamma} \right). \quad (91)$$

An important feature described by this expression is that λ vanishes at the frequency corresponding to the right edge of the photonic band gap, signifying the divergence of the respective penetration length. A similar effect takes place in MQW (Ref. 10) structures without the refractive index contrast. The important difference is that in the latter case the divergence occurs at the exciton frequency that lies at the center of the forbidden gap rather than at the band's boundary. Figure 7 shows the comparison of the solutions of the dispersion equation for different structures with the exciton homogeneous broadening taken into account.

D. MQW structures with complex elementary cells

In this section we illustrate the application of the developed technique to structures with complex elementary cells, which were first studied in Ref. 21. In that paper the mismatch between refractive indexes of different elements of the structure had to be neglected because the combination of the complex elementary cell and the spatial modulation of the refractive index turned out to be an insurmountable obstacle

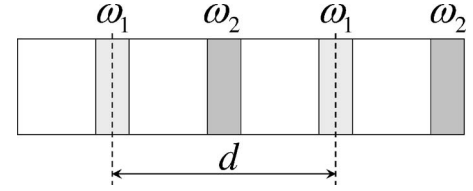


FIG. 8. The periodic structure with two QW's (dark rectangles) in the elementary cell. Dashed lines show the boundaries of the elementary cell having the mirror symmetry. The QW with the exciton frequency ω_2 is assumed to have an index of refraction different from other elements of the structure.

for the standard transfer matrix approach. In this section we show that the approach developed in the present paper allows us to overcome the technical difficulties associated with the consideration of a complex structure and to generalize the results of Ref. 21 for the case of structures with modulated refractive index.

We will focus here on one particular example, when the elementary cell consists of two QW's with different exciton frequencies ω_1 and ω_2 located half a period apart from each other (see Fig. 8). It was found in Ref. 21 that despite the presence of two different exciton frequencies, it is still possible to generalize the notion of the Bragg resonance for such systems and design structures whose spectrum would consist of only two polariton branches separated by a wide band gap. However, unlike the case of structures with a simple elementary cell, the formation of such a wide band gap requires not only the period of the structure to have a certain value, but also imposes a condition on the spectral separation between the excitonic frequencies of the wells constituting the elementary cell. When both generalized Bragg conditions are fulfilled for such a structure, the width of the polariton band gap, Δ_{CS} , becomes larger than that in the case of structures with a simple elementary cell:

$$\Delta_{CS} = \sqrt{2}\Delta_\Gamma. \quad (92)$$

This broadening of the gap by almost 40% reflects a possibility to effectively strengthen the exciton-photon interaction by increasing the density of QW's in the structure.

In this section we consider how the mismatch of the refractive indices affects the spectral properties of such structures. We simplify our consideration assuming that all elements of the structure except the wells with the exciton frequency ω_2 have the same refractive index. Formally, the dispersion equation describing modes propagating in such a structure in the normal direction has been obtained in Ref. 21 by more conventional methods, but that equation turned out to be too cumbersome to allow for any non-numerical analysis. Using the (a, f) representation of the transfer matrices, we show here that the dispersion equation can be rewritten in a much more transparent form with a factorized right-hand side.

To apply the technique developed in the present paper it is necessary to choose an elementary cell with explicit mirror symmetry. It can be done as shown in Fig. 8. The problem of determining the transfer matrices through the right and left halves of the QW can be resolved in the following way. We

note that the QW transfer matrix T_w determined by Eq. (55) can be written in a factorized form

$$T_w = T_b(\phi_w/2)\tilde{T}_w T_b(\phi_w/2), \quad (93)$$

where \tilde{T}_w is derived from the expression for T_w by setting $\phi_w=0$. After this factorization the transfer matrix through the elementary cell takes a form similar to Eq. (35):

$$T = \sqrt{\tilde{T}_w^{(1)}} T_b(\phi_b + \phi_w/2) T_\rho^{-1} T_w^{(2)} T_\rho T_b(\phi_b + \phi_w/2) \sqrt{\tilde{T}_w^{(1)}}. \quad (94)$$

The difference between the indices of refraction is again taken into account by introducing the special transfer matrix T_ρ , which describes the propagation of the wave across the interface and contains the respective Fresnel coefficients. The transfer matrices through different QW's, $T_w^{(1,2)}$, are obtained from Eq. (55) by substituting different excitonic susceptibilities

$$S_{1,2} = \frac{\Gamma_0}{\omega - \omega_{1,2} + i\gamma}. \quad (95)$$

The matrix square root $\sqrt{\tilde{T}_w^{(1)}}$ can be found to be equal to

$$\sqrt{\tilde{T}_w^{(1)}} = \begin{pmatrix} 1 - iS_1/2 & -iS_1/2 \\ iS_1/2 & 1 + iS_1/2 \end{pmatrix}. \quad (96)$$

Now, we can apply Eqs. (36), (37), and (39) to derive the (a, f) representation for T . The dispersion equation following from this representation has a relatively simple form

$$\cos^2\left(\frac{Kd}{2}\right) = \frac{1}{1 - \rho^2} [\text{Re}(a) + S_1 \text{Im}(a)][\text{Re}(b) + S_2 \text{Im}(b)], \quad (97)$$

where $a = \exp(i\phi_+) - \rho \exp(i\phi_-)$, $b = \exp(i\phi_+) + \rho \exp(i\phi_-)$ [compare with Eqs. (50)], and $\phi_\pm = \omega(2d_b n + d_w n \pm d_w n_2)/2c$.

As usual, the positions of band boundaries are determined by frequencies at which the RHS of Eq. (97) changes its sign, which can occur either by passing this expression through zero or through infinity. We can show that in the immediate proximity of the exciton frequencies, there are six band boundaries, which define three band gaps separated by two allowed bands. We again will be interested in finding conditions under which these allowed bands collapse, resulting in the formation of one continuous band gap. As we already know from the previously considered examples, the collapse of the allowed bands associated with the singularities of the exciton susceptibility S takes place when the exciton frequency coincides with one of the band boundaries of a certain effective structure. In the case of a simple elementary cell this effective structure was a respective passive photonic crystal; however, in the case under consideration, the effective structure is comprised of one of the sublattices of our system. More precisely, in order to cancel the exciton singularity at, for example, ω_1 , we have to require that ω_1 coincide with the zero of the expression inside the second set of parentheses on the RHS of Eq. (97). This zero, obviously, gives the position of some band boundaries of a structure made up of sublattice 2. Similarly, in order to cancel the

singularity at ω_2 we need to make it equal to one of the band boundaries originating from sublattice 1, particularly that which turns to zero the expression in the first set of parentheses of the RHS of Eq. (97). Let us assume for concreteness that $\omega_2 > \omega_1$; then, more specifically, we have to require that ω_1 be equal to the low-frequency boundary of the band gap associated with polariton branches in sublattice 2 and ω_2 should coincide with the high-frequency boundary of the band gap originating from polariton branches in sublattice 1. Let us denote the frequencies of these two band boundaries as $\omega_{1,2}^\pm$, where the lower index shows from which sublattice the respective boundary originates and \pm denotes high- and low-frequency boundaries, respectively. The frequencies $\omega_{1,2}^\pm$ can be found to be equal to

$$\omega_1^\pm = \frac{1}{2}(\omega_1 + \Omega_-) \pm \frac{1}{2}\sqrt{(\omega_1 - \Omega_-)^2 + \Delta_\Gamma^2},$$

$$\omega_2^\pm = \frac{1}{2}(\omega_2 + \Omega_+) \pm \frac{1}{2}\sqrt{(\omega_2 - \Omega_+)^2 + \Delta_\Gamma^2}, \quad (98)$$

where Ω_\mp are determined by Eqs. (52) and, for simplicity, we assumed the same value of the effective exciton-light interaction for both sublattices; i.e., we neglected a possible difference between exciton radiative decay rates in different wells. We also neglected the renormalization of Γ_0 due to the spatial modulation of the dielectric function [see Eqs. (70) and (84)]. The generalization of these expressions is straightforward but does not lead to anything new while making the resulting expressions much more cumbersome.

Let us, first, consider the case when the index of refraction of the wells of the second type is higher—i.e., $\rho > 0$. The conditions of absence of transparency windows inside the gap (the Bragg resonance conditions) are in this case formulated as $\omega_1^+ = \omega_2$ and $\omega_2^- = \omega_1$. Resolving these equations with respect to the exciton frequencies one obtains

$$\frac{\omega_1 + \omega_2}{2} = \Omega_c, \quad \omega_1 - \omega_2 = \frac{1}{2}(\sqrt{2\Delta_\Gamma^2 + \Delta_{PC}^2} - \Delta_{PC}), \quad (99)$$

which generalize the results of Ref. 21 to the case of structures with the refractive index mismatch. Substituting these results into the expression for the width of the band gap, which is equal to $\Delta = \omega_2^+ - \omega_1^-$, we obtain a familiar result

$$\Delta = \sqrt{\Delta_{CS}^2 + \Delta_{PC}^2}. \quad (100)$$

The case of $\rho < 0$ is described by the same formulas with the substitution $\Delta_{PC} \rightarrow -\Delta_{PC}$, which changes the Bragg condition [the second equation of Eqs. (99)] but leaves the width of the gap, Eq. (100), the same.

Thus, taking into account the mismatch of the indices of refraction in the system with a complex elementary cell leads to a modification of the Bragg condition in comparison with what one has in the case without a mismatch. This modification has a different character than in structures with a simple cell. The mean value of the exciton frequencies stays at the center of the forbidden gap, and only the difference between the frequencies must be corrected to take into ac-

count the mismatch. The resultant gap is, similar to the case of a simple cell, again the Pythagorean sum of the photonic and excitonic contributions.

IV. CONCLUSION

We considered the band structure associated with normal excitations of one-dimensional resonant photonic crystals using as a particular example exciton-polariton multiple-quantum-well structures. The properties of the normal modes of such structures are determined by the interplay of two mechanisms: the interaction of light with the internal resonances of the constituting materials, such as excitons in the MQW case, and multiple reflection of light due to periodic spatial modulation of the index of refraction of the structure. The necessity to take into account both mechanisms of the light-matter interaction in these structures on equal footing makes the analytical description of their properties more complicated than in the case of regular passive photonic crystals. In this paper we developed a powerful method of analyzing the band structure and dispersive properties of such structures, which allowed us to obtain analytical solutions for problems that could not be solved by other approaches.

This method is based on two key features. First, we construct transfer matrices using solutions of the appropriate Cauchy (rather than boundary value) problems as a basis. This makes calculations of the transfer matrices more convenient since it allows for avoiding difficult questions about the eigenmodes of the system under consideration. Second, we use a special representation of the transfer matrix valid for structures with an elementary cell possessing a mirror symmetry. This representation automatically yields the dispersion equation of normal modes in a factorized form, which drastically simplifies the analysis of the spectrum. In particular, using this representation we were able to analyze the dispersion properties of certain types of resonant photonic crystals with complex elementary cells. We also believe that besides the situations explicitly considered in this paper, the suggested method allows for an effective treatment of other problems such as exciton luminescence from MQW photonic crystals or for analysis of more complicated systems—e.g., quantum graphs.^{48,49} An important benefit of the developed approach consists also in the fact that polarization and angular dependences of the elements of transfer matrices appear in this approach only via respective Fresnel coefficients. This enabled us to obtain band structures of modes of both s and p polarizations in MQW-based photonic crystals from essentially the same dispersion equation and easily analyze their angular dependences.

We illustrated the developed method by applying it to a number of problems, some of which were considered previously in the framework of other approaches, while others were analyzed in this paper. In particular, we considered the polariton spectrum in several systems: MQW structures with mismatch of the indices of refraction of the barriers and wells materials, MQW with an arbitrary periodic modulation of the dielectric function, and MQW with a complex elementary cell consisting of two equidistant QW's characterized by

different exciton frequencies. We showed that in all these cases one can construct a structure, in which multiple photon and polariton bands can be collapsed in just two polariton branches separated by an anomalously broad stop band. Such a band structure is characteristic of so-called Bragg structures, which in the case of MQW's were studied in a number of previous publications. We showed here that in the case of RPC's with a simple elementary cell the condition for formation of such a spectrum can be formulated as a requirement for the exciton frequency to coincide with one of the edges of the respective passive photonic crystal. Formulated in this form this condition demonstrates a direct connection with earlier formulations of the Bragg resonance in MQW structures without the refractive index contrast. In the case of crystals with complex elementary cells, we showed that our method allows for taking into account the mismatch of the refractive indices between different elements of the structure and found the generalized Bragg conditions for this system as well. In the last case, this condition consists of two equations: one relating the period of the structure to the exciton frequencies of the constituent elements and the other specifying a relation between those frequencies.

One of the surprising results is that for all these structures the width of the polariton band gap in the case of the Bragg resonance can be presented in the form of a Pythagorean sum of the photonic and excitonic contributions, $\Delta^2 = \Delta_{PC}^2 + \tilde{\Delta}_{\Gamma}^2$. The excitonic contribution in the presence of the refractive index modulation, however, is modified compared to the case of simple optical lattices.

ACKNOWLEDGMENT

The work has been supported by AFOSR Grant No. F49620-02-1-0305.

APPENDIX: TRANSFER MATRIX FORMALISM

The transfer matrix technique has been reviewed in a number of publications. Here, however, we use this technique in a somewhat unusual form. Therefore, we find it useful to recall some important results. The general idea underlying the transfer matrix approach is to establish a linear relation between the solution of a differential equation taken at different points of space. More correctly, it is to provide an (irreducible) representation of the shift operator. While this idea is inherent to all formulations, the explicit form of the transfer matrix and its properties depend upon a choice of the basis for the representation. For a Sturm-Liouville problem, as such a basic one, one often chooses a 2×2 matrix operating on a two-dimensional vector, whose components are the value of a function, which represents a solution at a given point, and its derivative. The formal reason for this choice is the fact that a linear equation of a second order can always be reformulated as a system of two first-order equations for the function and its derivative, so one has

$$\begin{pmatrix} E(z+d) \\ E'(z+d) \end{pmatrix} = T_{\psi}(z+d, z) \begin{pmatrix} E(z) \\ E'(z) \end{pmatrix}. \quad (\text{A1})$$

Another approach to construct the transfer matrix is more convenient for problems involving the scattering of waves. This problem is most naturally described by specifying an amplitude of an incident wave and relating to it amplitudes of transmitted and reflected waves. In this approach, the field is sought in the form $e^{i\kappa z} + re^{-i\kappa z}$ at the one side of the system and in the form $te^{i\kappa z}$ at the other side. More generally, the field is represented in the form

$$E(z) = a_+ e^{i\kappa z} + a_- e^{-i\kappa z},$$

$$E(z+d) = a'_+ e^{i\kappa z} + a'_- e^{-i\kappa z}, \quad (\text{A2})$$

and the transfer matrix relates the amplitudes at the left and right boundaries:

$$\begin{pmatrix} a'_+ \\ a'_- \end{pmatrix} = T \begin{pmatrix} a_+ \\ a_- \end{pmatrix}. \quad (\text{A3})$$

As follows from Eqs. (A2), the transfer matrices written in representations (A1) and (A3) are related by a similarity transformation, $T = W_e^{-1}(z) T_\psi(z+d, z) W_e(z)$, where

$$W_e(z) = \begin{pmatrix} e^{i\kappa z} & e^{-i\kappa z} \\ i\kappa e^{i\kappa z} & -i\kappa e^{-i\kappa z} \end{pmatrix}. \quad (\text{A4})$$

Another important way to introduce the transfer matrix (see, e.g., Ref. 50) is based on a possibility of a representation of the solution of the Maxwell equation as a sum of two linearly independent functions $f_{1,2}(z)$, with modulated amplitudes

$$E(z) = c_1(z)h_1(z) + c_2(z)h_2(z),$$

$$E'(z) = c_1(z)h'_1(z) + c_2(z)h'_2(z). \quad (\text{A5})$$

Now, the transfer matrix gives the relation between the amplitudes at different points, usually a period of a structure apart,

$$\begin{pmatrix} c_1(z+d) \\ c_2(z+d) \end{pmatrix} = T_h(d) \begin{pmatrix} c_1(z) \\ c_2(z) \end{pmatrix}. \quad (\text{A6})$$

From Eq. (A5) it follows that

$$T_h(d) = W_h^{-1}(z+d) T_\psi(z+d, z) W_h(z), \quad (\text{A7})$$

where $W_h(z)$ is the Wronsky matrix:

$$W_h(z) = \begin{pmatrix} h_1(z) & h_2(z) \\ h'_1(z) & h'_2(z) \end{pmatrix}. \quad (\text{A8})$$

Equation (A8) allows one to derive a relation between transfer matrices obtained for a different choice of the basis functions $h_{1,2}$.

The relation between the transfer matrices written in the bases of plane waves and a pair of linearly independent functions can be written as²⁵

$$T = M(d/2) T_h(d) M^{-1}(-d/2), \quad (\text{A9})$$

where $M(z) = W_e^{-1}(0) W_h(z)$. Using Eqs. (A4), (A8), and (A9) one obtains

$$M(z) = \frac{1}{2} \begin{pmatrix} h_1(z) + \frac{h'_1(z)}{i\kappa} & h_2(z) + \frac{h'_2(z)}{i\kappa} \\ h_1(z) - \frac{h'_1(z)}{i\kappa} & h_2(z) - \frac{h'_2(z)}{i\kappa} \end{pmatrix}. \quad (\text{A10})$$

All types of transfer matrices have their advantages and disadvantages. For instance, a basis of a pair of linearly independent functions can be most naturally related to solutions of the Cauchy problem for the respective differential equation. Such a basis is easy to find but it is inconvenient for the solution of scattering problems. The fact that, generally, it is not related to T_ψ by a similarity transformation [see Eq. (A7)] makes it also difficult to consider spectral problems using this basis. Indeed, knowledge of the transfer matrix itself is not sufficient for solving this problem, and one has to separately consider a boundary value problem for amplitudes $c_{1,2}$. On the contrary, the basis of plane waves is the most suitable for solving this particular problem since the transfer matrix itself contains all needed information. In this basis, the difficulty of having to solve the boundary value problem is moved to the process of finding the transfer matrix itself. Therefore, the conversion rule from one basis to another presented in Eq. (A9) is very useful for practical calculations as is demonstrated in our paper.

¹E. Yablonovitch, Phys. Rev. Lett. **58**, 2059 (1987).

²S. John, Phys. Rev. Lett. **58**, 2486 (1987).

³J. D. Joannopoulos, R. D. Meade, and J. N. Winn, *Photonic Crystals: Molding the Flow of Light* (Princeton University Press, Princeton, 1995).

⁴R. Dicke, Phys. Rev. **93**, 99 (1954).

⁵I. H. Deutsch, R. J. C. Spreeuw, S. L. Rolston, and W. D. Phillips, Phys. Rev. A **52**, 1394 (1995).

⁶L. V. Keldysh, Superlattices Microstruct. **4**, 637 (1988).

⁷E. L. Ivchenko, A. I. Nesvizhskii, and S. Jorda, Phys. Solid State **36**, 1156 (1994).

⁸E. L. Ivchenko, Sov. Phys. Solid State **33**, 1344 (1991).

⁹M. Hübner, J. P. Prineas, C. Ell, P. Brick, E. S. Lee, G. Khitrova,

H. M. Gibbs, and S. W. Koch, Phys. Rev. Lett. **83**, 2841 (1999).

¹⁰L. I. Deych and A. A. Lisyansky, Phys. Rev. B **62**, 4242 (2000).

¹¹T. Ikawa and K. Cho, Phys. Rev. B **66**, 085338 (2002).

¹²V. Kuzmiak and A. A. Maradudin, Phys. Rev. B **55**, 7427 (1997).

¹³L. I. Deych, D. Livdan, and A. A. Lisyansky, Phys. Rev. E **57**, 7254 (1998).

¹⁴S. Nojima, Phys. Rev. B **61**, 9940 (2000).

¹⁵A. Y. Sivachenko, M. E. Raikh, and Z. V. Vardeny, Phys. Rev. A **64**, 013809 (2001).

¹⁶A. Christ, S. G. Tikhodeev, N. A. Gippius, J. Kuhl, and H. Gies-sen, Phys. Rev. Lett. **91**, 183901 (2003).

¹⁷K. C. Huang, P. Bienstman, J. D. Joannopoulos, K. A. Nelson, and S. Fan, Phys. Rev. Lett. **90**, 196402 (2003).

- ¹⁸O. Toader and S. John, Phys. Rev. E **70**, 046605 (2004).
- ¹⁹L. Pilozzi, A. D'Andrea, and K. Cho, Phys. Rev. B **69**, 205311 (2004).
- ²⁰E. L. Ivchenko, V. P. Kochereshko, A. V. Platonov, D. R. Yakovlev, A. Waag, W. Ossau, and G. Landwehr, Phys. Solid State **39**, 1852 (1997).
- ²¹E. L. Ivchenko, M. M. Voronov, M. V. Erementchouk, L. I. Deych, and A. A. Lisyansky, Phys. Rev. B **70**, 195106 (2004).
- ²²E. Ivchenko and A. Poddubny, Fiz. Tverd. Tela (S.-Peterburg) **48**, 540 (2006) [Phys. Solid State **48**, 561 (2006)].
- ²³M. V. Erementchouk, L. I. Deych, and A. A. Lisyansky, Phys. Rev. B **71**, 235335 (2005).
- ²⁴P. M. Morse and H. Feshbach, *Methods of Theoretical Physics* (McGraw-Hill, Tokyo, 1953), Vol. 1.
- ²⁵J. Mathews and R. L. Walker, *Mathematical Methods of Physics*, 2nd ed. (Benjamin/Cummings, Menlo Park, CA, 1970).
- ²⁶F. Tassone, F. Bassani, and L. C. Andreani, Phys. Rev. B **45**, 6023 (1992).
- ²⁷L. C. Andreani, G. Panzarini, A. V. Kavokin, and M. R. Vladimirova, Phys. Rev. B **57**, 4670 (1998).
- ²⁸S. Molchanov and B. Vainberg, J. Funct. Anal. **231**, 287 (2006).
- ²⁹B. A. Dubrovin, S. P. Novikov, and A. T. Fomenko, *Modern Geometry: Methods and Applications*, 2nd ed. (Springer, New York, 1992).
- ³⁰J. M. Bendickson, J. P. Dowling, and M. Scalora, Phys. Rev. E **53**, 4107 (1996).
- ³¹M. Born and E. Wolf, *Principles of Optics*, 7th ed. (Cambridge University Press, Cambridge, England, 1999).
- ³²A. Yariv and P. Yeh, *Optical Waves in Crystals* (Wiley, New York, 1984).
- ³³A. Kavokin and M. Kaliteevski, Solid State Commun. **95**, 859 (1995).
- ³⁴S. Haas, T. Stroucken, M. Hübner, J. Kuhl, B. Grote, A. Knorr, F. Jahnke, S. W. Koch, R. Hey, and K. Ploog, Phys. Rev. B **57**, 14860 (1998).
- ³⁵D. Ammerlahn, B. Grote, S. W. Koch, J. Kuhl, M. Hübner, R. Hey, and K. Ploog, Phys. Rev. B **61**, 4801 (2000).
- ³⁶L. C. Andreani, F. Tassone, and F. Bassani, Solid State Commun. **77**, 641 (1991).
- ³⁷D. S. Citrin, Phys. Rev. B **47**, 3832 (1993).
- ³⁸D. S. Citrin, Solid State Commun. **89**, 139 (1994).
- ³⁹S. Schmitt-Rink, D. Chemla, and D. Miller, Adv. Phys. **38**, 89 (1989).
- ⁴⁰J. P. Prineas, C. Ell, E. S. Lee, G. Khitrova, H. M. Gibbs, and S. W. Koch, Phys. Rev. B **61**, 13863 (2000).
- ⁴¹L. I. Deych, M. V. Erementchouk, and A. A. Lisyansky, Phys. Rev. B **69**, 075308 (2004).
- ⁴²J. Winn, Y. Fink, S. Fan, and J. Joannopoulos, Opt. Lett. **23**, 1573 (1998).
- ⁴³D. Chigrin, A. Lavrinenko, D. Yarotsky, and S. Gaponenko, Appl. Phys. A: Mater. Sci. Process. **68**, 25 (1999).
- ⁴⁴A. Bruyant, G. Lerondel, P. Reece, and M. Gal, Appl. Phys. Lett. **82**, 3227 (2003).
- ⁴⁵T. Yonte, J. Monzon, A. Felipe, and L. Sanchez-Soto, J. Opt. A, Pure Appl. Opt. **6**, 127 (2004).
- ⁴⁶Z. Yang, N. Kwong, R. Binder, and A. Smirl, J. Opt. Soc. Am. B **22**, 2144 (2005).
- ⁴⁷Z. Yang, N. Kwong, R. Binder, and A. Smirl, Opt. Lett. **30**, 2790 (2005).
- ⁴⁸P. Kuchment, Waves Random Media **12**, R1 (2002).
- ⁴⁹P. Kuchment, Waves Random Media **14**, S107 (2004).
- ⁵⁰R. Perez-Alvarez, C. Trallero-Herrero, and F. Garcia-Moliner, Eur. J. Phys. **22**, 275 (2001).
- ⁵¹It raises a question is it possible to have both $\varphi_{1,2}$ equal to 0. Generally, the answer is positive, since any finite set of linearly independent functions spans only a subspace of functions integrable with square. However, it can be seen that it is impossible for the exciton in a ground state and for all frequencies below the first photonic band gap. Thus, the latter is always affected by the exciton-light interaction. This impossibility can be proven also for all frequencies for the model considered here of symmetric quantum wells and spatial modulation of the dielectric function. The same result stands for δ -functional approximation for the envelope wave function. These results make the question about the possibility for the effective exciton-light interaction to be completely inhibited rather academic.